

Axion search with optical technique.

Ryszard Stroynowski¹ and Ariel R. Zhitnitsky²

Southern Methodist University, Dallas, Texas 75275, USA.

Abstract

A brief review of particle physics motivations for axion existence is followed by a discussion of optical observables that can be used for axion detection. It is emphasised that the resonant photon - axion transition can occur in the presence of low density gas bringing the experimentally accessible quantities within the reach of the present day technology.

¹E-mail: ryszard@mail.physics.smu.edu.

² On leave of absence from Budker Institute of Nuclear Physics, Novosibirsk, 630090
Russia
E-mail: arz@smuphy.physics.smu.edu.

1. Introduction.

Recently, there has been a renewed interest [1] in the possibility of searching for light pseudoscalar particles using laser interferometry. This interest has been stimulated by the availability of SSC and other magnets for non accelerator applications. The idea of using of the optical techniques to measure vacuum birefringence in the presence of strong magnetic fields and to search for scalar and pseudoscalar particles was originally proposed by Iacopini and Zavattini [2] and has been extensively reviewed and discussed by several authors mainly in the context of the search for solar axions [3], [4],[5],[6],[7]. A discussion of the QED tests can be found in [8]. First application of this technique was made by an experiment of Cameron et al., [9] which used laser interferometry to measure optical rotation of light polarization in a magnetic field and was able to estimate a limit for the axion coupling to two photons $g_{a\gamma\gamma} < 3.6 \cdot 10^{-7} \text{ GeV}^{-1}$ for axion masses $m_a < 10^{-3} \text{ eV}$.

In this note we first briefly discuss the particle physics motivations for the existence of axions and then review the experimental observables and their limitations for axion detection with optical techniques. A complete axion - photon mixing formula is derived without any approximations. A resonant photon-axion transition in the presence of low density gas enhances the values of measurable quantities and suggests a novel experimental approach. It is shown that, in the resonant case, present technology can reach theoretically expected limits of the photon-axion coupling constant for axion masses $m_a \geq 10^{-3} \text{ eV}$. Astrophysical arguments constraining axion properties have been extensively reviewed elsewhere [10].

2. Review of axion physics.

2.1 The strong CP problem

The axion is generally thought to be the most attractive solution to the strong CP problem. We begin by first formulating the problem.

The general Lagrangian for a renormalizable, gauge invariant quantum field theory that includes only fundamental gauge field A_μ with spin 1 (photons, gluons...) and fields of matter q^i with spin 1/2 can be written as:

$$L = \frac{-1}{4} F_{\mu\nu} F^{\mu\nu} + \sum_{i=flavor} \bar{q}^i (i\gamma_\mu D_\mu - m^i) q^i + \frac{g^2 \theta}{32\pi^2} \tilde{F}^{\mu\nu} F_{\mu\nu} \quad (1)$$

Here,

$$D_\mu = \partial_\mu - igA_\mu$$

is a covariant derivative, g is the coupling constant,

$$F_{\mu\nu} \equiv \frac{-1}{ig} [D_\mu, D_\nu]$$

is the strength tensor of the gauge field and

$$\tilde{F}_{\mu\nu} = \frac{1}{2}\epsilon_{\mu\nu\lambda\sigma}F^{\lambda\sigma}$$

is the dual of the field strength tensor. The third term in the Lagrangian, characterized by the strength θ , is a total derivative; it affects neither the equations of motion, nor the perturbative aspects of the theory.

In the case of Quantum Electrodynamics the coupling constant g should be identified with electric charge and A_μ with photon field. Because QED is a purely perturbative theory, the theta term can be disregarded since it does not contribute to any observable quantity.

In the Standard Model of electroweak interactions, some nonperturbative effects might occur. However, their contributions, characterized by the θ term, are proportional to $e^{-\frac{2\pi}{\alpha}}$, where the fine structure constant $\alpha \equiv \frac{g^2}{4\pi} = \frac{1}{137}$. This proportionality factor is a very small number and can be neglected in general discussions.

In the case of strong interactions, the coupling g in the formula (1) is related to a strong coupling constant α_s via $\alpha_s = \frac{g^2}{4\pi}$; the field A_μ should be identified with an octet of gluon fields and $F_{\mu\nu}$ is the strength tensor of the gluon field. Because of a large value of the strong coupling constant α_s , this term should have, in principle, a significant contribution. In fact, in QCD it can be proven that the observable quantities depend on θ .

The existence of the θ term implies a violation of P, CP and T symmetries. However, there is no experimental evidence for P or CP violation in strong interactions. For example, CP violation in QCD would induce electric dipole moments of strongly interacting particles and there are stringent experimental limits on those quantities. Thus the absence of CP violating effects in QCD indicates a very small value for the parameter θ . The most restrictive upper limit on its value can be derived from the experimental bound [11] on the neutron electric dipole moment: $d < 12 \cdot 10^{-26}$ e-cm at 95 % CL. The corresponding upper limit on θ is [12]:

$$\theta \leq 10^{-9}. \tag{2}$$

Now we are ready to formulate the problem: why is θ so small?

There are several possible answers to this question. The most elegant one was proposed by Peccei and Quinn who assumed that the strong interactions Lagrangian has a global $U_{PQ}(1)$ chiral symmetry [13]. Weinberg and Wilczek [14] analysed the consequences of the Peccei-Quinn symmetry and noticed that the spontaneous breaking of a global chiral symmetry $U_{PQ}(1)$ leads to a light pseudoscalar pseudo-Goldstone boson, called an axion, that will interact with topological charge.

To see, how the existence of a $U_{PQ}(1)$ symmetry automatically leads to the effective $\theta_{eff} = 0$ let us introduce into theory a new scalar field $\phi(x)$

in such a way that, under a $U_{PQ}(1)$ transformation, the quark and ϕ fields transform as:

$$\phi \rightarrow e^{i\alpha} \phi, \quad q_i \rightarrow e^{-i\alpha\gamma_5/2} q_i. \quad (3)$$

In other words, we allow for existence of an additional complex scalar field, which must be included in the Lagrangian. In this case, the phase of the new field cancels exactly the original θ parameter. The price for this cancellation is an appearance of a new particle - the axion a .

The axion couples to all constituents of matter - quarks and gluons. The coupling strength to fermions is proportional to $\frac{m_q}{f_a}$, where m_q represents a quark mass and f_a is a dimensional parameter describing the energy scale of the Peccei-Quinn symmetry breaking. All physical observables can be expressed in terms of f_a . For example, the axion's interactions with gluons are described by a triangle diagram, shown in Fig.1 and are given by

$$L_{agg} = \frac{g^2}{32\pi^2} \tilde{F}^{\mu\nu a} F_{\mu\nu}^a \left(\frac{a}{f_a} \right). \quad (4)$$

These interactions mix the axion with the neutral pion through the gluons, yielding an effective low-energy axion potential. It generates an axion mass in analogy to the way in which the chiral symmetry breaking generates a mass for the π meson.

2.2 Axion mass

The axion mass is related to the QCD scale parameter via

$$m_a \sim \Lambda_{QCD}^2 / f_a,$$

where Λ_{QCD} represents a scale of strong interactions physics and is of the order of 100 MeV.

Originally, f_a was thought to be the same as the symmetry-breaking scale of the weak interactions, i.e., about 250 GeV. As a consequence the axion mass was expected to be of the order of 100 keV. This type of axion has been ruled out early by particle decay and beam dump experiments. However, allowing the Peccei-Quinn symmetry breaking scale f_a to become much larger results in an axion with much lower mass and a weaker coupling to matter. Models for such "invisible axions" include the Dine-Fischler-Srednicki-Zhitnitsky (DFSZ) axion [15] which couples to all fermions and the Kim-Shifman-Vainshtein-Zakharov (KSVZ) axion [16] which couples to quarks only.

For invisible axions there are no a priori bounds on f_a . However, one can calculate the relevant properties of this particle in terms of f_a . The axion mass comes from the mixing of the axion with the neutral pion. Thus the axion mass is proportional to $1/f_a$ and to the neutral pion parameters: its mass $m_\pi = 135$ MeV and its decay constant $f_\pi = 133$ MeV. The exact

relation is given by [10]:

$$m_a = \frac{f_\pi m_\pi}{f_a} \frac{\sqrt{m_u m_d}}{(m_u + m_d)} \simeq 0.6 \cdot 10^{-5} eV \left(\frac{10^{12} GeV}{f_a} \right) \quad (5)$$

where m_u and m_d represent masses of up and down quarks making up the neutral pion. For the numerical estimate we assume $m_u = 4$ MeV and $m_d = 7$ MeV.

2.3 Axion interactions

The most important quantity for us is the coupling of the axion to two photons, described by the coupling constant $g_{a\gamma\gamma}$, which can be derived from the axion-fermion interactions. There are two independent contributions to $g_{a\gamma\gamma}$. One of them comes from interactions with leptons (electrons, muons and taus) through a triangle loop. Because the axion coupling with fermions is proportional to $1/f_a$ and is very small, $g_{a\gamma\gamma}$ is small. This contribution is exactly zero for the KSVZ model, in which the axion-lepton interactions are absent. The second - a hadronic contribution - is related to the mixing of axion with π^0 meson. The exact formula [10] for $g_{a\gamma\gamma}$ is given by:

$$g_{a\gamma\gamma} = \frac{\alpha}{2\pi f_a} \cdot \left(\frac{N_l}{N} - \frac{5}{3} - \frac{m_d - m_u}{m_d + m_u} \right), \quad (6)$$

where $g_{a\gamma\gamma}$ is defined by the following Lagrangian of photon - axion interactions:

$$L_{a\gamma\gamma} = \frac{g_{a\gamma\gamma}}{4} \tilde{F}_{\mu\nu} F_{\mu\nu} \cdot a = -\frac{1}{M} \vec{E} \cdot \vec{B} a. \quad (7)$$

Here, we see explicit relation of the Lagrangian to the electric field \vec{E} and the magnetic field \vec{B} . The axion interacts only with the photon wave component parallel to an external magnetic field. The energy scale M is defined as

$$M \equiv \frac{1}{g_{a\gamma\gamma}}.$$

In the above definitions, N_l is a constant proportional to the number of charged leptons and the factor N is an analogous constant related to the number of gluons. For each model these constants can be explicitly calculated. The ratio $\frac{N_l}{N}$ differs from model to model. In the DFSZ model, as well as in all grand unified axion models, the value of the ratio $\frac{N_l}{N}$ is [10]:

$$\frac{N_l}{N} = \frac{8}{3}.$$

In the (KSVZ) model there are no axion interactions with leptons ($N_l = 0$). Therefore, the relative strength of the axion-photon-photon coupling in the two models is given by ξ :

$$\xi \equiv \frac{g_{a\gamma\gamma}(DFSZ)}{g_{a\gamma\gamma}(KSVZ)} = \frac{\frac{8}{3} - \frac{5}{3} - \frac{m_d - m_u}{m_d + m_u}}{-\frac{5}{3} - \frac{m_d - m_u}{m_d + m_u}} \simeq -0.37. \quad (8)$$

Bearing in mind that all observable values depend on $g_{a\gamma\gamma}^2$ we conclude that KSVZ-axion interactions are $\xi^{-2} \simeq 7$ times stronger than DFSZ-axion interactions.

Equations (5) and (6) also show that the axion mass m_a and axion-photon coupling constant M^{-1} are not independent parameters, but are related to each other by:

$$m_a M(\text{DFSZ}) = 7.4 \cdot 10^{18} \text{eV}^2, \rightarrow \left(\frac{m_a \text{eV}}{10^{-5}}\right) \left(\frac{M \text{GeV}}{10^{15}}\right) = 0.74 \quad (9)$$

$$m_a M(\text{KSVZ}) = 2.7 \cdot 10^{18} \text{eV}^2 \rightarrow \left(\frac{m_a \text{eV}}{10^{-5}}\right) \left(\frac{M \text{GeV}}{10^{15}}\right) = 0.27 \quad (10)$$

A priori the axion mass window spans the range 10^{-12} eV to 10^6 eV. Laboratory experiments searched without success for axions with mass $m_a > 10$ keV in the decays $K^+ \rightarrow \pi^+ + a$, $J/\psi \rightarrow a + \gamma$, $\Upsilon \rightarrow a + \gamma$ and others. Both high-mass and low-mass axions are constrained by astrophysical arguments originally advanced by Dicus *et al.*, [17] and extensively discussed in excellent reviews [10]. Present understanding of the evolution of red giants eliminates the window of $10^{-2} \text{eV} < m_a < 10^5 \text{eV}$ while the observed duration of the neutrino burst from the SN1987A supernova eliminates $10^{-3} \text{eV} < m_a < 2$ eV. Very low mass axions with $m_a < 10^{-6}$ eV are excluded by cosmological considerations. The main window of axion mass still allowed is in the range $10^{-6} \text{eV} \leq m_a \leq 10^{-3} \text{eV}$.

2.4 Axion lifetime

The axion width for decay into two photons is defined by the axion-photon interaction (7) and is given by

$$\Gamma(a \rightarrow \gamma\gamma) = \frac{g_{a\gamma\gamma}^2 m_a^3}{64\pi}. \quad (11)$$

Its lifetime depends on its mass (or on the symmetry breaking scale M):

$$\tau(a \rightarrow \gamma\gamma) \sim 5 \cdot 10^{49} \left(\frac{M \text{ GeV}}{10^{15} \text{ GeV}}\right) s, \quad (12)$$

which is sufficiently long to have no effect on our observations.

3. Definitions of observables.

In order to define the relations between the physical processes involved in light propagation in a magnetic field and the observable quantities, let us consider a light wave, with an amplitude \vec{A} and angular frequency ω , that initially is linearly polarized at an angle ϕ with respect to an external magnetic field \vec{B} :

$$\vec{A} = \vec{i} \cos \phi + \vec{j} \sin \phi, \quad (13)$$

where \vec{i} is unit vector parallel to $B_{ext}^{\vec{}}$, \vec{j} is orthogonal to $B_{ext}^{\vec{}}$ and \vec{k} is the direction of propagation. At a time t the amplitude can be expressed as:

$$\vec{A} = (\vec{i}A_{\parallel}(t) \cos \phi + \vec{j}A_{\perp}(t) \sin \phi)e^{-i(\omega t - \omega \vec{k}z)}. \quad (14)$$

The propagation of light in the magnetic field is affected by several different processes. The most significant is a pure, second order in α , QED process of Delbruck scattering off the virtual photons coupled to virtual electron loops shown in Fig.2. This is a process in which the vacuum can be treated as a sea of virtual electron-positron pairs. In an external magnetic field these pairs become polarized and the resulting polarized electric field interferes with the electric field of a propagating photon. The interference affects the parallel and perpendicular components differently and results in a change of the polarization of the light wave. This effect is referred to as the QED vacuum birefringence and it is derived from the Heisenberg effective Lagrangian [18]:

$$L = \frac{-1}{4}F_{\mu\nu}F_{\mu\nu} + \frac{\alpha^2}{90m_e^4}[(F_{\mu\nu}F_{\mu\nu})^2 + \frac{7}{4}(\tilde{F}_{\mu\nu}F_{\mu\nu})^2] \quad (15)$$

The same Lagrangian can be expressed in terms of explicit electric and magnetic fields:

$$L = \frac{1}{2}(\vec{E}^2 - \vec{B}^2) + \frac{2\alpha^2}{45m_e^4}[\vec{E}^4 + \vec{B}^4 - 2\vec{E}^2\vec{B}^2 + 7(\vec{E} \cdot \vec{B})^2] \quad (16)$$

Another process which may influence the light propagation is related to photon - axion interactions. Equation (7), describing these interactions, contains a dot product of the electric and magnetic fields. Therefore, a photon with its electric field \vec{E} polarized in the direction parallel to an external magnetic field $B_{ext}^{\vec{}}$ can produce axions. A photon with \vec{E} polarized perpendicular to the magnetic field remains unaffected. For example, if a light beam enters the magnetic field region with its linear polarization at an angle with respect to the magnetic field direction, its parallel component A_{\parallel} is attenuated and undergoes a change of phase (because of axion production), while its orthogonal component remains the same.

Neglecting effects that are even higher order in α , we can use an approximate expression for the parallel component of the amplitude, $A_{\parallel}(t)$, that separates the phase shift of the wave from its attenuation:

$$A_{\parallel}(t) = (1 + \epsilon_{\parallel}(t) + i\varphi_{\parallel}(t)). \quad (17)$$

$$A_{\perp}(t) = (1 + i\varphi_{\perp}(t)) \quad (18)$$

In this representation $\epsilon(t)$ describes the attenuation and $\varphi_{\parallel}(t)$ and $\varphi_{\perp}(t)$ are related to the phase shift. The physical quantities that can be measured are:

ellipticity: $\psi = \frac{1}{2}|\varphi_{\parallel}(t) - \varphi_{\perp}(t)| \sin 2\phi$

rotation: $\varepsilon = \frac{1}{2}|\epsilon_{\parallel}(t)| \sin 2\phi$.

The ellipticity describes the ratio of the minor and major axes of the photon polarization vector. It depends on the phase shift of the light wave and is generated by both the pure QED and photon-axion interference. The rotation refers to a rotation of the photon polarization vector after the passage through the magnetic field. It depends on the wave attenuation only and cannot be generated by pure QED processes. Polarized light propagating over a path length l through a transverse magnetic field will gain an ellipticity due to Delbruck scattering given by:

$$\psi_{QED} = \frac{\alpha^2 B_{ext}^2 l \omega}{15m_e^4}. \quad (19)$$

$$\varepsilon_{QED} = 0. \quad (20)$$

If the light passes through the same magnetic field N times, the corresponding formula for ellipticity is:

$$\psi_{QED} = \frac{\alpha^2 B_{ext}^2 l \omega N}{15m_e^4}. \quad (21)$$

Here, and throughout the paper, we use a unit system in which $\hbar = c = 1$. In this system the length and magnetic field units can be expressed in terms of eV:

$$1m = 5 \cdot 10^6 \text{ eV}^{-1}$$

$$1T = 195 \text{ eV}^2$$

It is often convenient to present these results in terms of refractive indices n_{\perp} and n_{\parallel} which refer to the transverse and parallel polarization of the wave with respect to an external magnetic field.

$$n_{\perp} = \frac{c}{\text{velocity of transverse wave}} \equiv 1 + \frac{\Delta_{\perp}}{\omega} \quad (22)$$

and

$$n_{\parallel} = \frac{c}{\text{velocity of parallel wave}} \equiv 1 + \frac{\Delta_{\parallel}}{\omega}. \quad (23)$$

Here, the index of refraction is defined [19] by the relation between the photon momentum k and its frequency ω

$$k = n \cdot \omega, \quad (24)$$

where the velocity of light in vacuum is $c = 1$. In terms of Δ_{\parallel} and Δ_{\perp} the ellipticity is given by $\psi = \frac{1}{2} \frac{|\Delta_{\parallel} - \Delta_{\perp}|}{\omega} \sin 2\phi$.

In practice, a perfect vacuum does not exist. Therefore the Δ_{\parallel} and Δ_{\perp} terms in the above equations should be extended to represent total refractive indices that include both vacuum and residual gas contributions. We shall use the notation Δ^{vac} , Δ^{gas} , introduced in ref.[7], for the vacuum and gas contributions respectively. Δ^{gas} is a function of density, temperature, chemical composition of the gas, and magnetic field strength. In an external magnetic field $\Delta_{\parallel}^{gas} \neq \Delta_{\perp}^{gas}$, and the difference contributes to the so called Cotton-Mouton effect of birefringence in gasses and liquids in a magnetic field. The effect can be accounted for by a Cotton-Mouton constant C defined by

$$\frac{\Delta_{\parallel}^{gas} - \Delta_{\perp}^{gas}}{\omega} = n_{\parallel}^{gas} - n_{\perp}^{gas} = C\lambda B_{ext}^2, \quad (25)$$

where λ is the wavelength of the light.

4. Axion-photon mixing.

We are ready now to formulate the result for photon-axion mixing in an external field B . The axion mixes only with a photon component that is parallel to an external magnetic field. The physical states resulting from the mixing are linear combinations of the axion and the parallel component of the photon wave:

$$\begin{aligned} A'_{\parallel} &= A_{\parallel} \cos \vartheta + a \sin \vartheta \\ a' &= -A_{\parallel} \sin \vartheta + a \cos \vartheta. \end{aligned}$$

The strength of the mixing is characterized by a mixing angle ϑ [7]:

$$\frac{1}{2} \tan(2\vartheta) = \frac{B}{2M(\Delta_{\parallel} - \Delta_a)}. \quad (26)$$

The parameter Δ_a is related to the axion mass and photon frequency by

$$\Delta_a = -\frac{m_a^2}{2\omega}.$$

The sign of the Δ_a comes from the dispersion relation

$$k = \sqrt{\omega^2 - m_a^2} \simeq \omega \left(1 - \frac{m_a^2}{2\omega^2}\right).$$

Finally, we can introduce a concept of oscillation length described by: $\frac{2\pi}{\Delta_{osc}}$, where $\Delta_{osc} = \Delta_{\parallel} - \Delta_a$. The mixing angle ϑ in most cases is very small.

We will now discuss the effects on the light observables - ellipticity and rotation - from the axion-photon mixing. We discuss the case in which light propagates in a magnetic field of length l . In some experiments, light bounces N times through the length l and the corresponding effects increase linearly with N .

4.1 Axion-photon mixing in vacuum.

We follow calculations presented by Raffelt and Stodolsky [7]. The axion contribution to ellipticity is:

$$\psi_a = \frac{1}{2} \frac{\omega^2 B_{ext}^2 N}{M^2 m_a^4} (\gamma - \sin \gamma). \quad (27)$$

Here, γ is a dimensionless parameter relating path length, mass of the axion and the angular frequency of the photon:

$$\gamma \equiv \frac{m_a^2 l}{2\omega}.$$

The analogous formula for rotation is:

$$\varepsilon_a = \frac{\omega^2 B_{ext}^2 N}{M^2 m_a^4} \cdot \sin^2\left(\frac{\gamma}{2}\right), \quad (28)$$

where γ is given above. For $\gamma \ll 1$, which occurs for small axion masses and relatively short magnetic field length, one can expand the above formulae (27, 28) to get simple approximate expressions:

$$\psi_a = \frac{m_a^2 B_{ext}^2 l^3 N}{96\omega M^2}, \quad \gamma \ll 1 \quad (29)$$

$$\varepsilon_a = \frac{l^2 B_{ext}^2 N}{16M^2}, \quad \gamma \ll 1. \quad (30)$$

4.2 Axion-photon mixing in media.

Up to now we discussed axion-photon mixing in vacuum, where the effect is weak. The mixing is more complicated for photon propagation through a medium. In that case we have to use a complete formula for the mixing. General expressions for the axion-photon mixing contributions to the ellipticity and rotation can be derived following the same method as used by Raffelt and Stodolsky [7] but without the small mixing angle approximation. The complete solution is obtained by diagonalization of the mixing matrix:

$$\varepsilon = \varepsilon_{QED} + \frac{1}{2} \left[1 - \cos^2 \vartheta \cos\left(\frac{Bl}{2M} \tan \vartheta\right) - \sin^2 \vartheta \cos\left(\frac{Bl}{2M} \cot \vartheta\right) \right] \quad (31)$$

$$\psi = \psi_{QED} + \frac{1}{2} \left[\cos^2 \vartheta \sin\left(\frac{Bl}{2M} \tan \vartheta\right) - \sin^2 \vartheta \sin\left(\frac{Bl}{2M} \cot \vartheta\right) \right] \quad (32)$$

In what follows, we explore the regions of mixing angle in which mixing effects are largest.

For small values of the mixing angle, $\vartheta \ll 1$, we can use the approximation

$$\frac{1}{2} \tan(2\vartheta) \simeq \vartheta$$

and the formulae for the ellipticity and rotation in terms of ϑ are analogous to previous discussed equations (27) and (28):

$$\psi_a = \frac{\vartheta^2 N}{2} [\Delta_{osc} l - \sin(\Delta_{osc} l)] \quad (33)$$

$$\varepsilon_a = \vartheta^2 N \sin^2(\Delta_{osc} l/2) \quad (34)$$

where

$$\vartheta = \frac{B}{2M\Delta_{osc}} \ll 1$$

and

$$\Delta_{osc} = \Delta_{\parallel}^{vac} + \Delta_{\parallel}^{gas} - \Delta_a \simeq \frac{m_a^2}{2\omega}$$

4.3 Resonant case.

Another region of interest is the axion-photon resonance, which occurs when $\Delta_{\parallel} \simeq \Delta_a$. In vacuum the signs of the pure QED and axion contributions are opposite $\Delta_{\parallel}^{vac} > 0$ and $\Delta_a < 0$ and their difference is always positive. However, in a gas medium with a plasma frequency much smaller than the photon frequency, the light scattering contribution is negative $\Delta_{\parallel}^{gas} < 0$. In such case it is possible to obtain a cancellation in the denominator of the Eq. (26) when $\Delta_{\parallel} - \Delta_a = \Delta_{\parallel}^{vac} + \Delta_{\parallel}^{gas} - \Delta_a = 0$. This corresponds to a resonant condition $\vartheta = 45^\circ$. In the ideal resonance case the expression for the rotation is given by

$$\varepsilon_a = \frac{1}{2} (1 - \cos(\frac{Bl}{2M})) \simeq \frac{1}{4} (\frac{Bl}{2M})^2 \quad (35)$$

The photon-axion transition probability is given by

$$P(\gamma_{\parallel} \rightarrow a) = \sin^2(\frac{Bl}{2M}). \quad (36)$$

All these formulae should be multiplied by a factor N for multiple-beam-path experiments. From these formulae it is seen that if we had the length $l_{ocs} \sim \frac{\pi M}{B}$, complete transition between photons and axions would occur.

The resonant case provides an important handle on axion detection with optical interferometry. Naively, one can expect that an increase in the light propagation path length l through the magnetic field, would increase the values of observable quantities. This is true for ellipticity from a pure QED process (see eq.(19)). It is also true for ellipticity from the axion contribution (see eq.(33)), which is almost ten order of magnitude smaller than that from QED and thus difficult to observe. However, the rotation ε_a is free from the QED corrections. The expression derived for the rotation dependence on the length shows an oscillatory behaviour with increasing value of l . This is illustrated in Fig. 3, where the expected value for the rotation is plotted as function of the length parameter l for axion mass of 10^{-4} eV for the case of

a possible experiment with no additional medium discussed in the following section. As can be seen, even the most optimistic values of the rotation are very small and are well below experimentally accessible range. Thus, the only avenue open to experimentation is the case of the resonant transition.

The resonance condition for the photon-axion mixing requires that the axion and the photon waves are coherent in the the volume with nonzero magnetic field. For axions with mass $m_a \neq 0$, this coherence condition requires the presence of Δ_{gas} and can be achieved by filling the region where magnetic field is present with an appropriate medium. In such a case the photon acquires an effective mass m_γ which can be made to match m_a giving a resonance condition

$$m_a = m_\gamma.$$

For short wavelength, i.e., energetic photons, the dispersion relation is given [19] by

$$k^2 = \omega^2 - m_\gamma^2,$$

where m_γ plays the role of the plasma frequency in the medium:

$$m_\gamma^2 = \frac{4\pi\alpha N_e}{m_e}.$$

Here, N_e is the electron density and m_e is the electron mass. In general, the effective photon mass in a gas can be expressed in terms of atomic scattering amplitudes and we refer the reader to the corresponding literature [6], [20] on this subject. The electron density, N_e , is proportional to the gas pressure, P , and inverse temperature, T^{-1} , so we can rewrite the resonant condition in terms of the gas pressure. The normalization has to be provided by a measurement. For example, for helium gas at room temperature and at 1 atm pressure m_γ was found [6] to be ~ 0.3 eV. The scaling relation gives

$$P = 1atm \cdot \left(\frac{m_a}{0.3}\right)^2 \cdot \left(\frac{T}{300K}\right). \quad (37)$$

For an axion with mass $m_a = 10^{-4}$ eV, the helium pressure generating a resonance condition at temperature $T \simeq 4K$ is $P \simeq 10^{-6}$ Torr (see Fig.4). The above formula is applicable only in the limit $\omega \gg m_\gamma$, which is satisfied for any laser with frequency ω of order few eV. ³ The difference between resonant and non-resonant conditions is illustrated in Fig.5, where the expected value of optical rotation plotted as function of the axion mass for the two cases and for the same values of external magnetic field, photon energy and path length. As can be seen, the rotation in the resonant case does not show the oscillatory character and can reach higher values for axion mass above

³An analogous idea has been discussed for the solar axion search experiment [5]. The only difference is the range of the axion mass, which in that case was considered to be about few eV. The required gas pressure was in the range of 0.1 – 300 atm. Because of the high energy of solar axions (about few keV) the condition $\omega \gg m_\gamma$ was also satisfied.

10^{-3} eV. This is due to the expected increase of the photon - axion coupling constant with increase of the axion mass. As a result, the size of an effect is much enhanced in the resonant case bringing the observable quantities within reach of present day technology. An experiment to search for axions can be performed by a scan of the gas pressure in the magnetic volume.

The resonant condition can be maintained so long as the photon mass is close to the axion mass with the required precision given by the relation

$$\frac{m_a - m_\gamma}{m_a} \ll \frac{2\omega}{lm_a^2}. \quad (38)$$

This formula depends strongly on the mass. For example, a search for an axion with $m_a \simeq 10^{-3}$ eV requires adjusting gas pressure and temperature with about 10% accuracy. Searching for axions with larger masses requires better accuracy.

5. Numerical estimates

In this section we discuss the numerical estimates for the experiment recently completed by the Brookhaven - Rochester - Fermilab - Trieste group, in which the laser light passed up to 250 times through two dipole magnets providing an average magnetic field value of 2.15 Tesla, and compare them to a proposed experiment using 10 SSC dipoles of the Accelerator Sector String Test facility (ASST) with a field of 6.76 Tesla and total active length of 150 meters.

5.1 Brookhaven-Rochester-Fermilab-Trieste experiment

We start with discussion of the Rochester - Brookhaven - Fermilab - Trieste experiment of Cameron et al.[9] The relevant parameters are:

$$l = 8.8m, \quad N = 250, \quad B_{ext}^2 = 4.5T^2, \quad \omega = 2.41eV. \quad (39)$$

For these parameters, the value of γ ,

$$\gamma = \left(\frac{m_a}{0.33 \cdot 10^{-3} eV} \right)^2, \quad (40)$$

is small for the mass range $m_a < 10^{-4}$ eV and we can use the approximate expressions (29) and (30). In the absence of systematic errors, the expected values of the ellipticity and rotation are:

$$\psi_{QED} \simeq 0.24 \cdot 10^{-12}$$

$$\psi_a = 1.57 \cdot 10^{-22} \frac{\left(\frac{m_a eV}{10^{-3}}\right)^2}{\left(\frac{MGeV}{10^{13}}\right)^2}, \quad \gamma \ll 1. \quad (41)$$

$$\varepsilon_a = 5 \cdot 10^{-23} \frac{1}{\left(\frac{M\text{GeV}}{10^{13}}\right)^2}, \quad \gamma \ll 1. \quad (42)$$

For an axion mass $m_a = 10^{-4}$ eV which corresponds to a symmetry breaking scale $M=0.74 \cdot 10^{14}$ GeV in DFSZ model, we expect $\psi_a = 3 \cdot 10^{-26}$ and $\varepsilon_a = 9 \cdot 10^{-25}$. These values are illustrated in Fig.6. They are exceedingly small, well beyond the reach of the experiment.

5.2 ASST experiment

In the initial stage of the ASST experiment we expect to have 10 SSC dipole magnets operating at nominal field value and a long wavelength laser with light bouncing 1000 times through the magnetic field:

$$l = 150m, \quad N = 1000, \quad B_{ext} = 6.76T, \quad \omega = 1.17eV(\lambda = 1.06\mu m). \quad (43)$$

The QED expectation for the ellipticity is then

$$\psi_{QED} \simeq 0.8 \cdot 10^{-10}.$$

For most of the interesting axion mass window, the parameter γ is of order of one

$$\gamma = \left(\frac{m_a}{5.5 \cdot 10^{-5}eV}\right)^2 \sim 1, \quad (44)$$

and we have to use the exact equation (27). The calculated ellipticity due to photon - axion mixing is about 10 orders of magnitude smaller than that from the QED effects:

$$\psi_a = 0.8 \cdot 10^{-20}, \quad \gamma \gg 1. \quad (45)$$

The estimate of rotation depends on the axion model. For the DFSZ axion it is given by:

$$\varepsilon_a(DFSZ) = 0.41 \cdot 10^{-18} \frac{\sin^2(\gamma/2)}{\left(\frac{m_a eV}{10^{-5}}\right)^2}, \quad \gamma \sim 1. \quad (46)$$

Here, we assumed the relation (9) between the axion mass and the photon coupling constant.

For the KSVZ axion model the, interaction is stronger and the formula (46) should be multiplied by a factor ξ^{-2} :

$$\varepsilon_a(KSVZ) = 3 \cdot 10^{-18} \frac{\sin^2(\gamma/2)}{\left(\frac{m_a eV}{10^{-5}}\right)^2}, \quad \gamma \sim 1. \quad (47)$$

These values are illustrated in Fig.7 for the resonant and non-resonant cases.

At a later stage of the project we expect to increase the number of times a photon traverses the magnetic field, to increase the field value to 10 T and to use frequency doubling:

$$l = 150m, N = 10000, B_{ext} = 10T, \omega = 2.34eV(\lambda = 0.53\mu m). \quad (48)$$

In this case QED predicts ellipticity

$$\psi_{QED} \simeq 0.35 \cdot 10^{-8}.$$

In vacuum, the photon-axion interaction effect gives the ellipticity

$$\begin{aligned} \psi_a(DFSZ) &= 0.35 \cdot 10^{-18} \\ \psi_a(KSVZ) &= 2.5 \cdot 10^{-18} \end{aligned}$$

and rotation

$$\varepsilon_a(DFSZ) = 0.36 \cdot 10^{-16} \frac{\sin^2(\gamma/2)}{\left(\frac{m_a eV}{10^{-5}}\right)^2}, \quad \gamma \sim 1. \quad (49)$$

$$\varepsilon_a(KSVZ) = 2.6 \cdot 10^{-16} \frac{\sin^2(\gamma/2)}{\left(\frac{m_a eV}{10^{-5}}\right)^2}, \quad \gamma \sim 1. \quad (50)$$

The corresponding values in the resonant case are much higher and are illustrated in Fig.8. Preliminary estimates of the measurement precision of the ellipticity and rotation indicate [21] a possibility of reaching the expected axion limits for $m_a \geq 10^{-3}$ eV.

6. Conclusions.

There is a strong motivation for existence of the axion from particle physics arguments. Experiments designed for axion detection face difficulties associated with its expected small mass and weak coupling to other particles. The resonant photon - axion transition allows for an application of an optical detection method that uses laser interferometry in a magnetic field to explore the axion mass range $m_a \geq 10^{-3}$ eV.

Acknowledgements.

The authors acknowledge helpful discussions with F. Nezrick and are grateful for careful reading of the manuscript and critical comments by V. Teplitz.

References

- [1] T. C. Chui et al., Proposal to Measure the Velocity of Light in a Magnetic Field. Submitted to US Department of Energy (1994);
K. Van Bibber et al., Phys. Rev. Letters **59**, (1987), 759;
D. Bakalov et al., Nucl. Phys. **B** (Proc. Suppl.) **35**, (1994), 180.

- [2] E. Iacopini and E. Zavattini, Phys. Letters **B85**, (1979), 151.
- [3] P. Sikivie, Phys. Rev. Letters **51**, (1983), 1415; *ibid* **52**, (1984), 695.
- [4] L. Maiani, R. Petronzio and E. Zavattini, Phys. Letters **175**, (1986), 359.
- [5] D. E. Morris, LBL Report No. LBL-19594, 1985;
K. Van Bibber et al., Fermilab Letter of Intent P794, 1988;
K. Van Bibber et al., Phys. Rev. **D39**, (1989), 2089.
- [6] D. M. Lazarus et al. Phys. Rev. Letters **69**, (1992), 2333.
- [7] G. Raffelt and L. Stodolsky, Phys. Rev. **D37**, (1988), 1237.
- [8] Wei-Tou Ni et al., Mod. Phys. Letters **A6**, (1991), 3671.
- [9] R. Cameron et al., Phys. Rev. **D47**, (1993), 3707.
- [10] J. E. Kim, Phys. Reports **150**, (1987), 1;
H. Y. Cheng, Phys. Reports **158**, (1988), 1;
R. D. Peccei, in *CP violation*, C. Jarlskog ed., World Scientific, 1989,
pp 503-551;
M. S. Turner, Phys. Reports **197**, (1990), 67;
G. G. Raffelt, Phys. Reports **198**, (1990), 1.
- [11] Review of Particle Properties, Phys. Rev. **D45**, (1992), 1.
- [12] R. Grewther, P. DiVecchia, G. Veneziano, E. Witten, Phys. Letters **B88**,
(1979), 123.
- [13] R. D. Peccei and H. Quinn, Phys. Rev. Letters **38**, (1977), 1440.
- [14] S. Weinberg, Phys. Rev. Letters **40**, (1978), 223;
F. Wilczek, Phys. Rev. Letters **40**, (1978), 279.
- [15] M. Dine, W. Fischler and M. Srednicki, Phys. Letters **B104**, (1981), 199;
A. Zhitnitsky, Yad.Fiz. **31**, (1980), 497 (Sov.J.Nucl. Phys. **31**, (1980),
260).
- [16] J. E. Kim, Phys. Rev. Letters **43**, (1979), 103;
M. A. Shifman, A. I. Vainshtein and V. I. Zakharov, Nucl. Phys. **B166**,
(1980) 493.
- [17] D. A. Dicus, E. W. Kolb, V. L. Teplitz and R. V. Wagoner, Phys. Rev.
D18, (1978), 1829.
- [18] W. Heisenberg and H. Euler, Z. Phys. **98**, (1936), 714.

- [19] J. D. Jackson, *Classical Electrodynamics*, Wiley, New York, 1975, 2nd Ed., p. 288-302.
- [20] B. L. Henke et al. *At. Data Nucl. Data Tables* **27**, (1982), 1.
- [21] M. Shao, private communication.

Figure Captions.

Fig. 1. QCD triangle diagram for axion - gluon interactions.

Fig. 2. Feynman diagram for photon scattering in an external magnetic field.

Fig. 3. Rotation as function of the photon path length for the second stage of the ASST experiment with following parameters $m_a = 10^{-4}$ eV, $B=6.76$ T, $N=10000$, and $\omega = 2.34$ eV.

Fig. 4. Helium pressure as function of the axion mass at temperature of 4 K for the resonant transition case.

Fig. 5. Rotation as function of axion mass for the same experimental parameters as in Fig.3 and $l = 150m$ for the non-resonant and resonant case.

Fig. 6. Ellipticity and rotation for the Brookhaven - Rochester - Fermilab - Trieste experiment a) ellipticity, b) rotation, non-resonant case, c) rotation, resonant case.

Fig. 7. Ellipticity and rotation for the first stage of the ASST experiment a) ellipticity, b) rotation, non-resonant case, c) rotation, resonant case.

Fig. 8. Ellipticity and rotation for the second stage of the ASST experiment a) ellipticity, b) rotation, non-resonant case, c) rotation, resonant case.

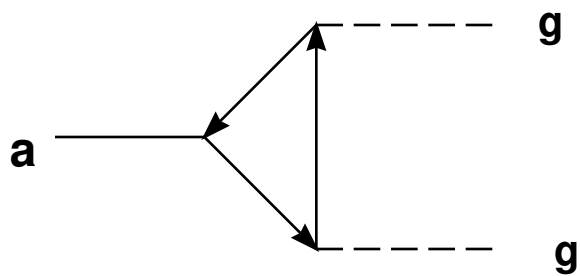


Fig.1

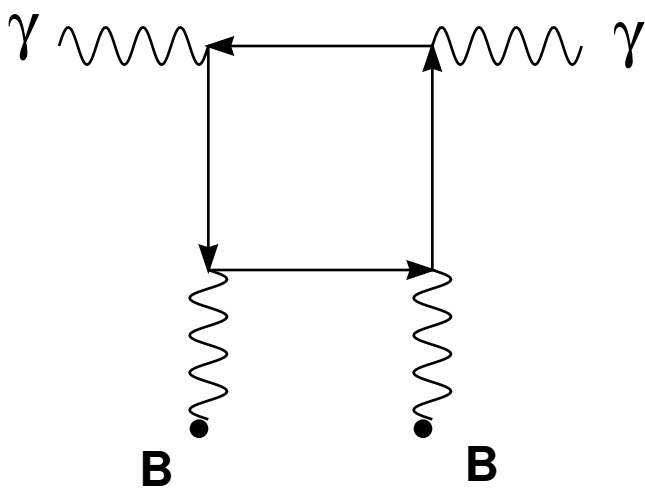


Fig.2

This figure "fig1-1.png" is available in "png" format from:

<http://arxiv.org/ps/hep-ph/9409251v1>

This figure "fig2-1.png" is available in "png" format from:

<http://arxiv.org/ps/hep-ph/9409251v1>

This figure "fig1-2.png" is available in "png" format from:

<http://arxiv.org/ps/hep-ph/9409251v1>

This figure "fig2-2.png" is available in "png" format from:

<http://arxiv.org/ps/hep-ph/9409251v1>

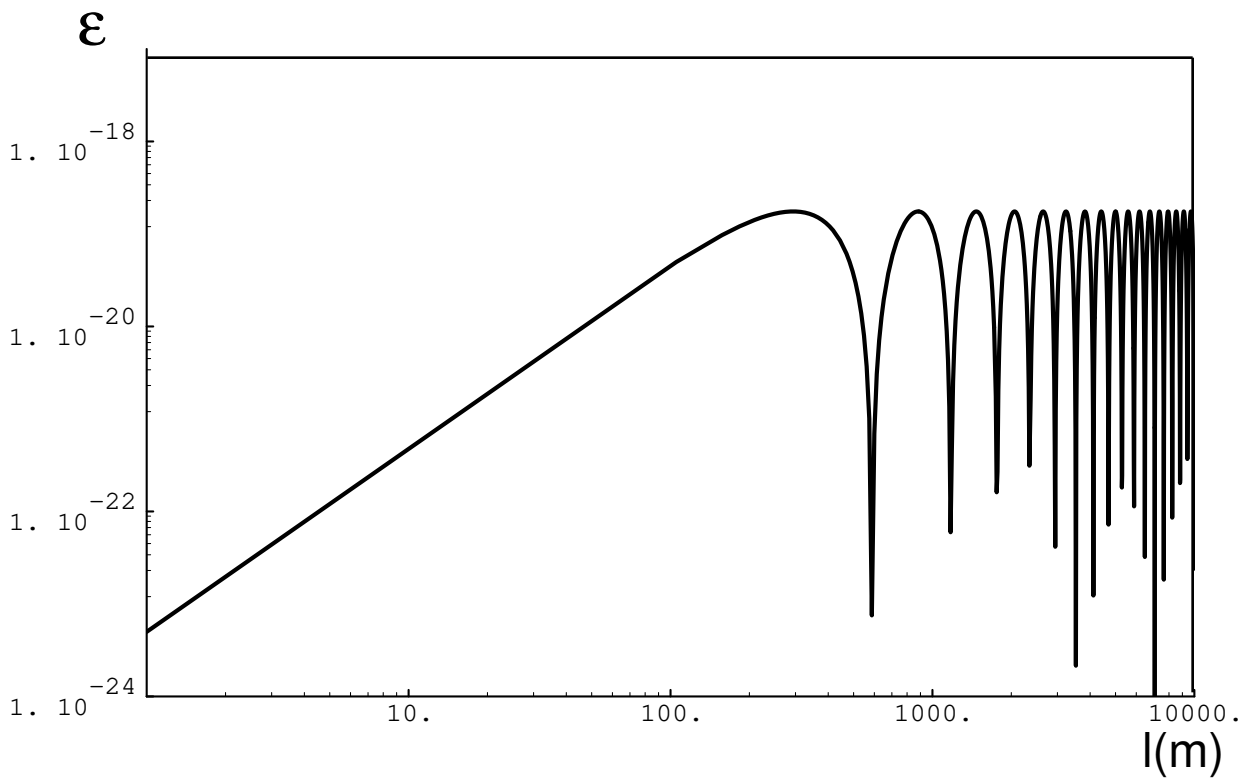


Fig.3

This figure "fig1-3.png" is available in "png" format from:

<http://arxiv.org/ps/hep-ph/9409251v1>

This figure "fig2-3.png" is available in "png" format from:

<http://arxiv.org/ps/hep-ph/9409251v1>

pressure
(Torr)

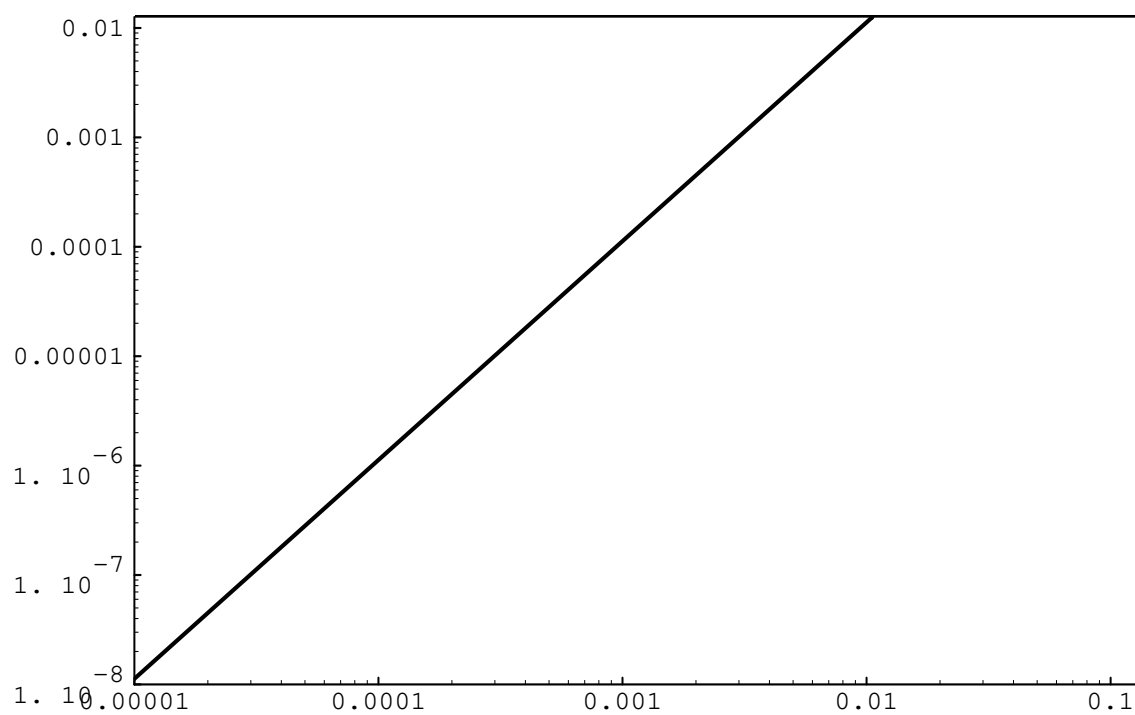


Fig.4

m(eV)

This figure "fig1-4.png" is available in "png" format from:

<http://arxiv.org/ps/hep-ph/9409251v1>

This figure "fig2-4.png" is available in "png" format from:

<http://arxiv.org/ps/hep-ph/9409251v1>

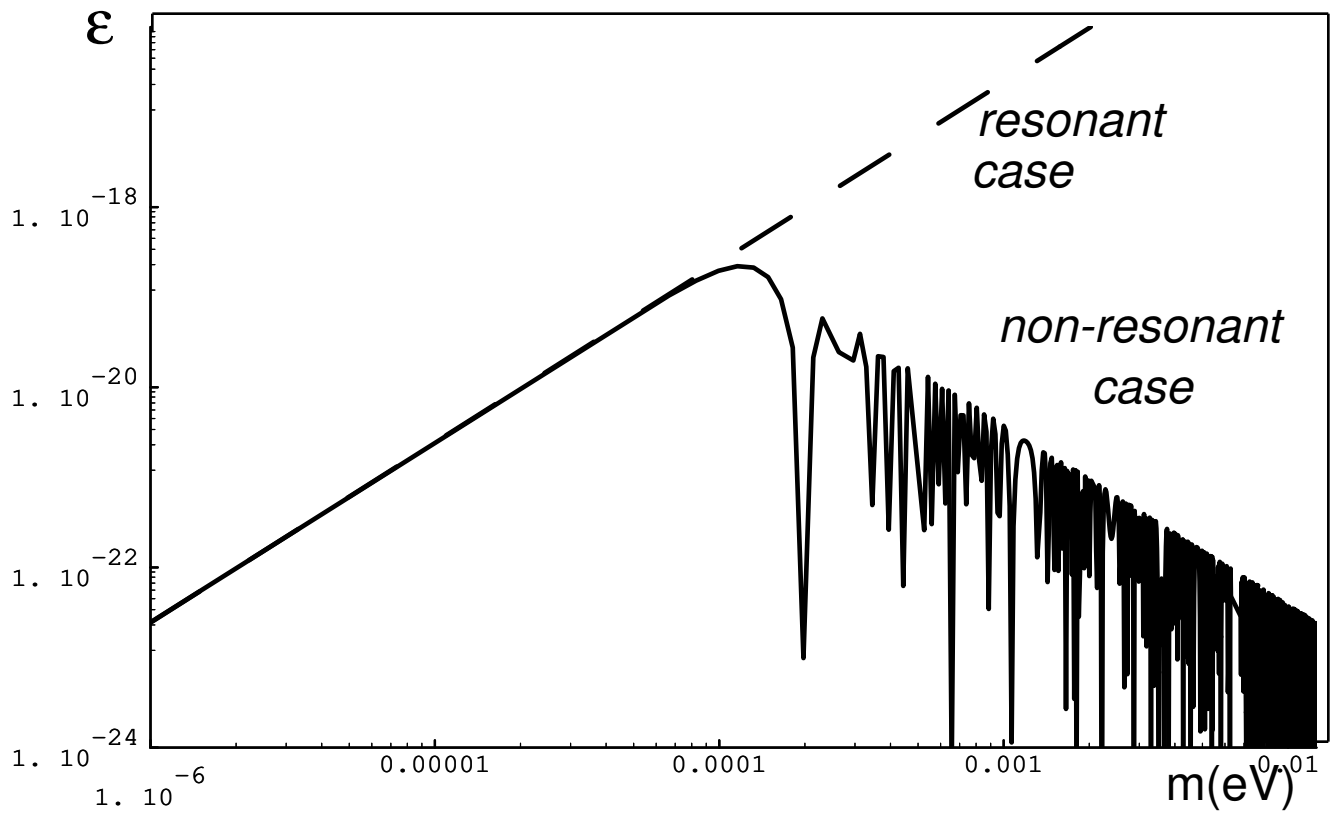


Fig.5

This figure "fig1-5.png" is available in "png" format from:

<http://arxiv.org/ps/hep-ph/9409251v1>

This figure "fig2-5.png" is available in "png" format from:

<http://arxiv.org/ps/hep-ph/9409251v1>

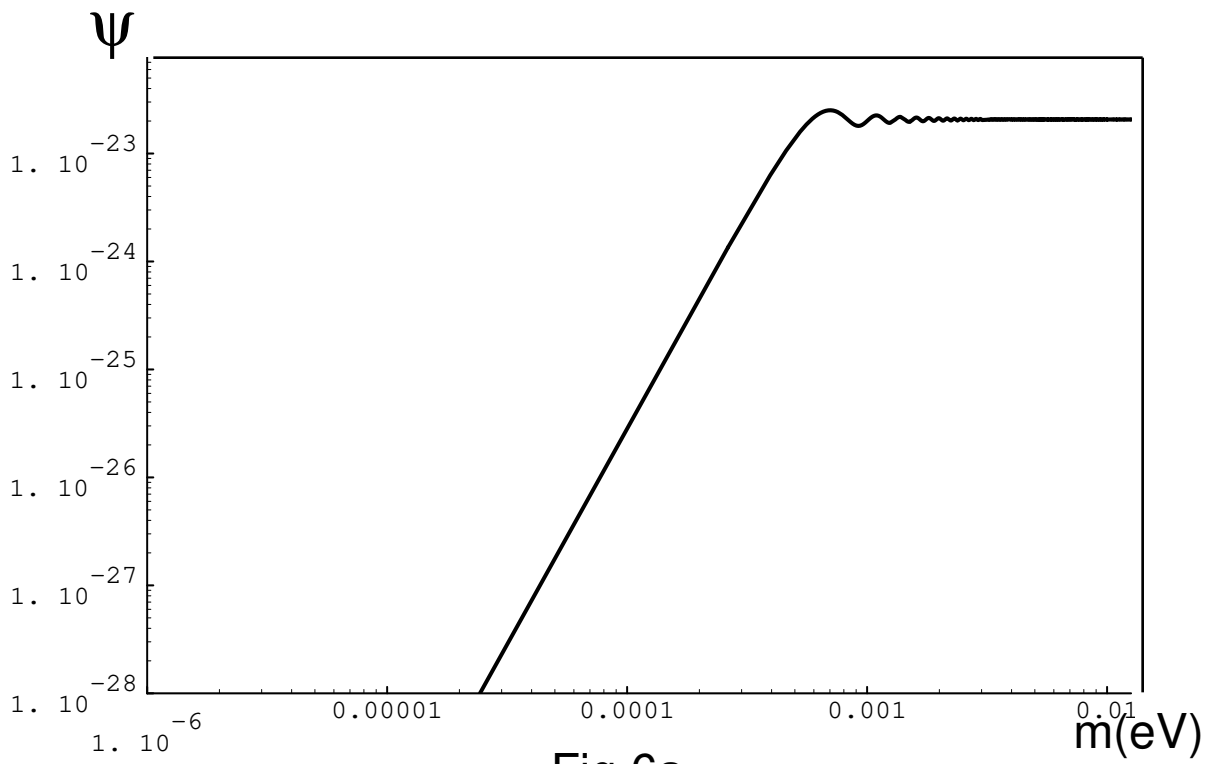


Fig.6a

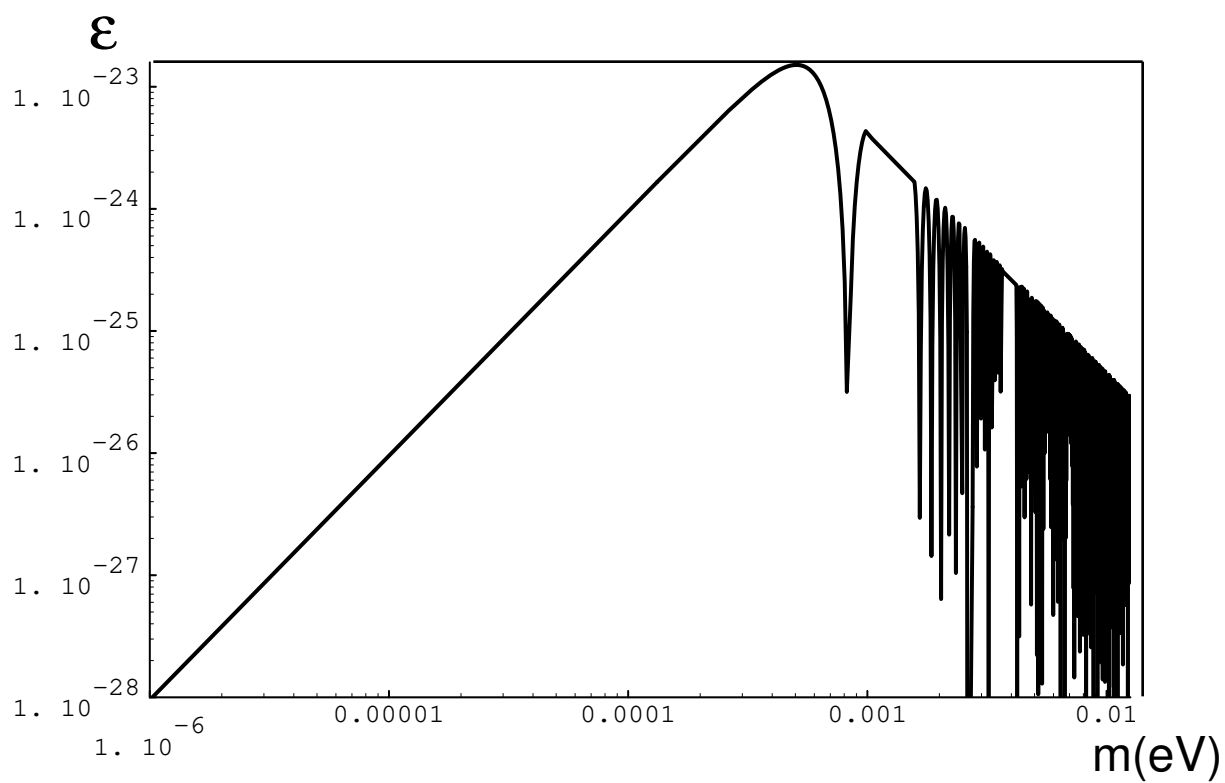


Fig.6b

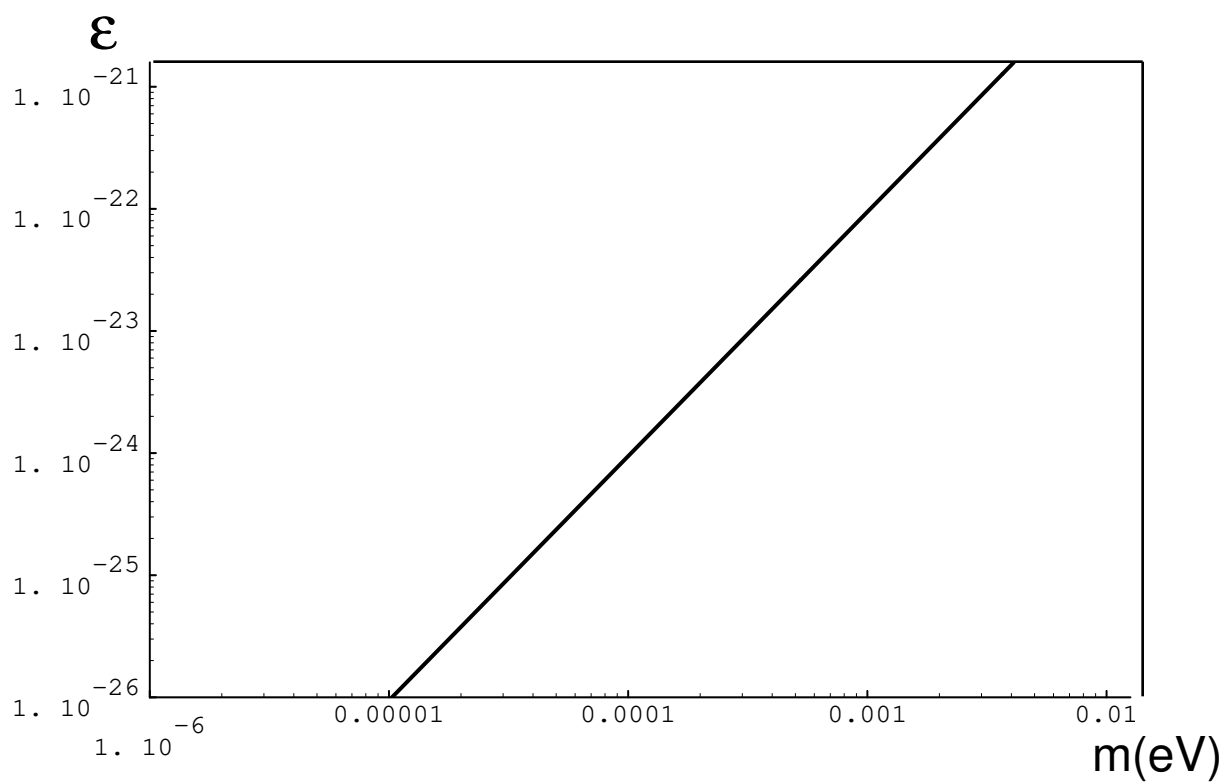


Fig.6c

This figure "fig1-6.png" is available in "png" format from:

<http://arxiv.org/ps/hep-ph/9409251v1>

This figure "fig2-6.png" is available in "png" format from:

<http://arxiv.org/ps/hep-ph/9409251v1>

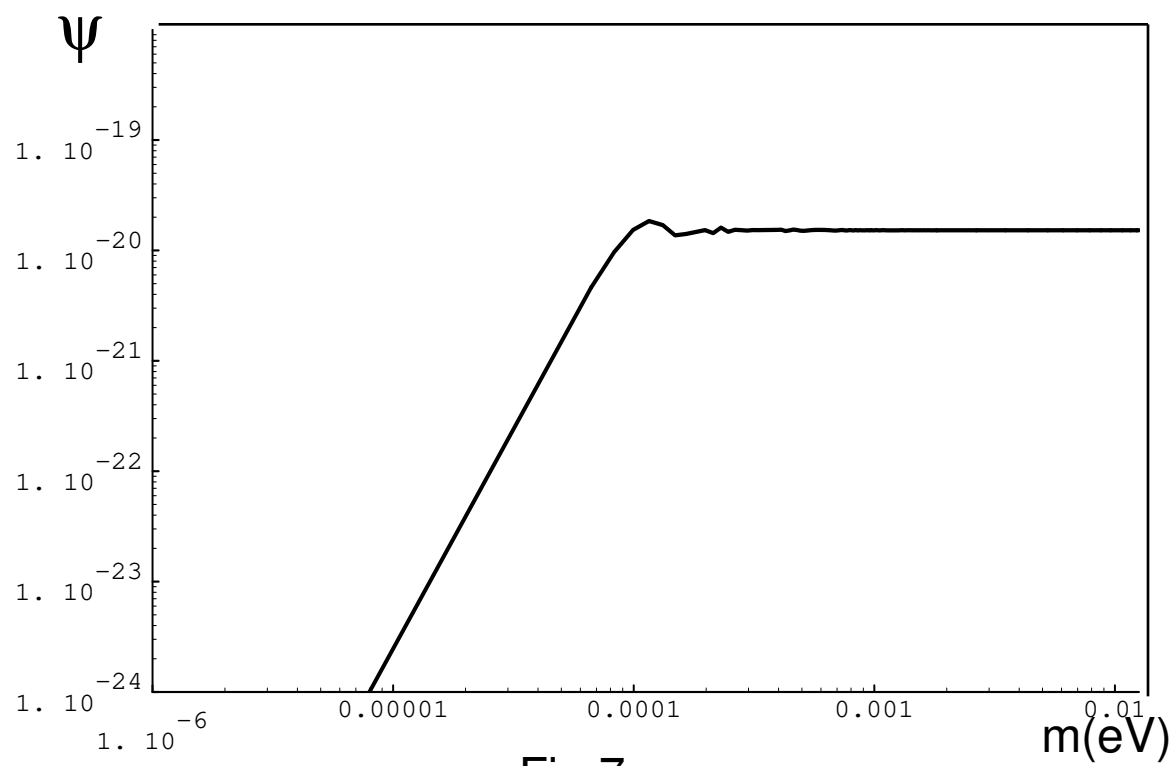


Fig.7a

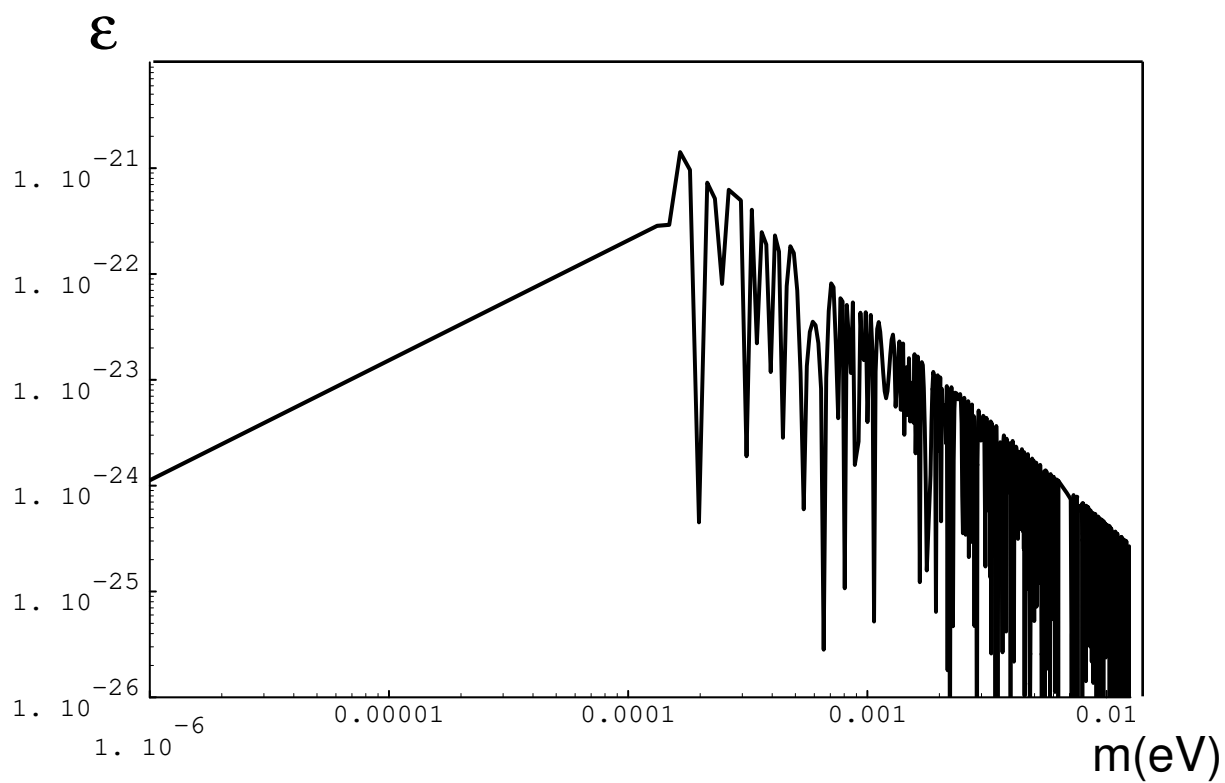


Fig.7b

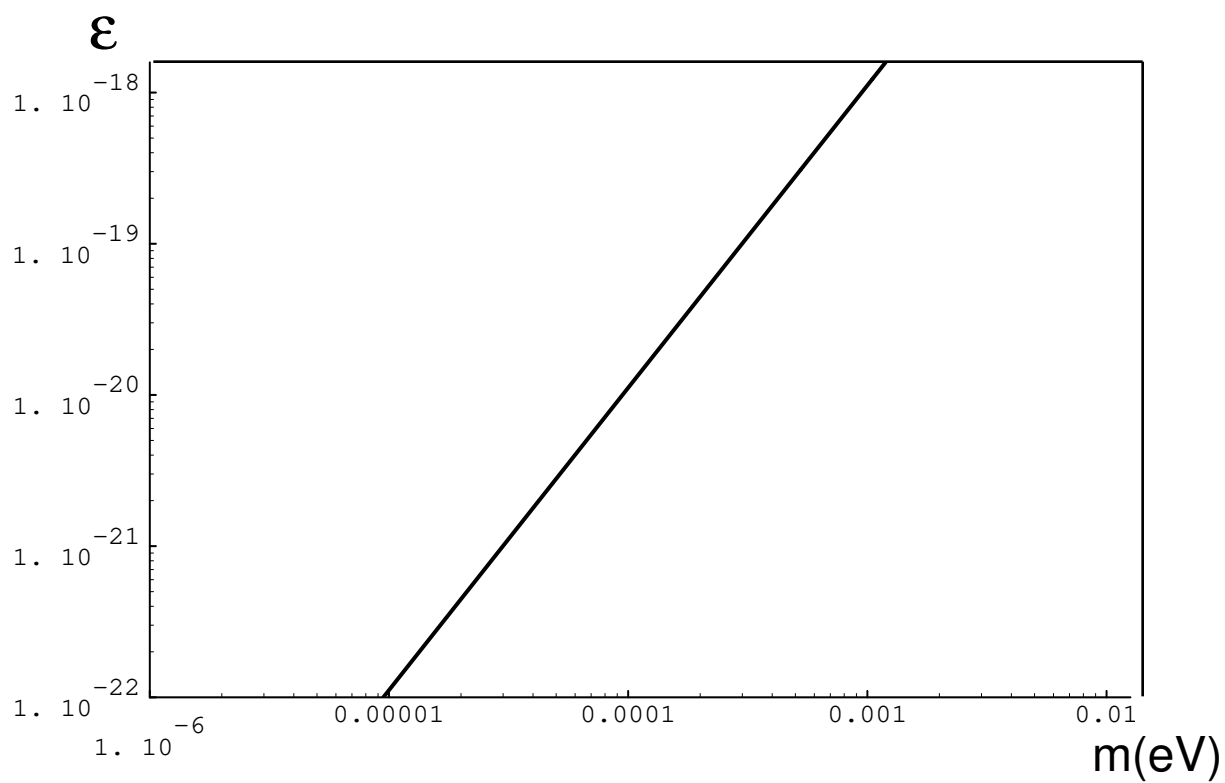


Fig.7c

This figure "fig1-7.png" is available in "png" format from:

<http://arxiv.org/ps/hep-ph/9409251v1>

This figure "fig2-7.png" is available in "png" format from:

<http://arxiv.org/ps/hep-ph/9409251v1>

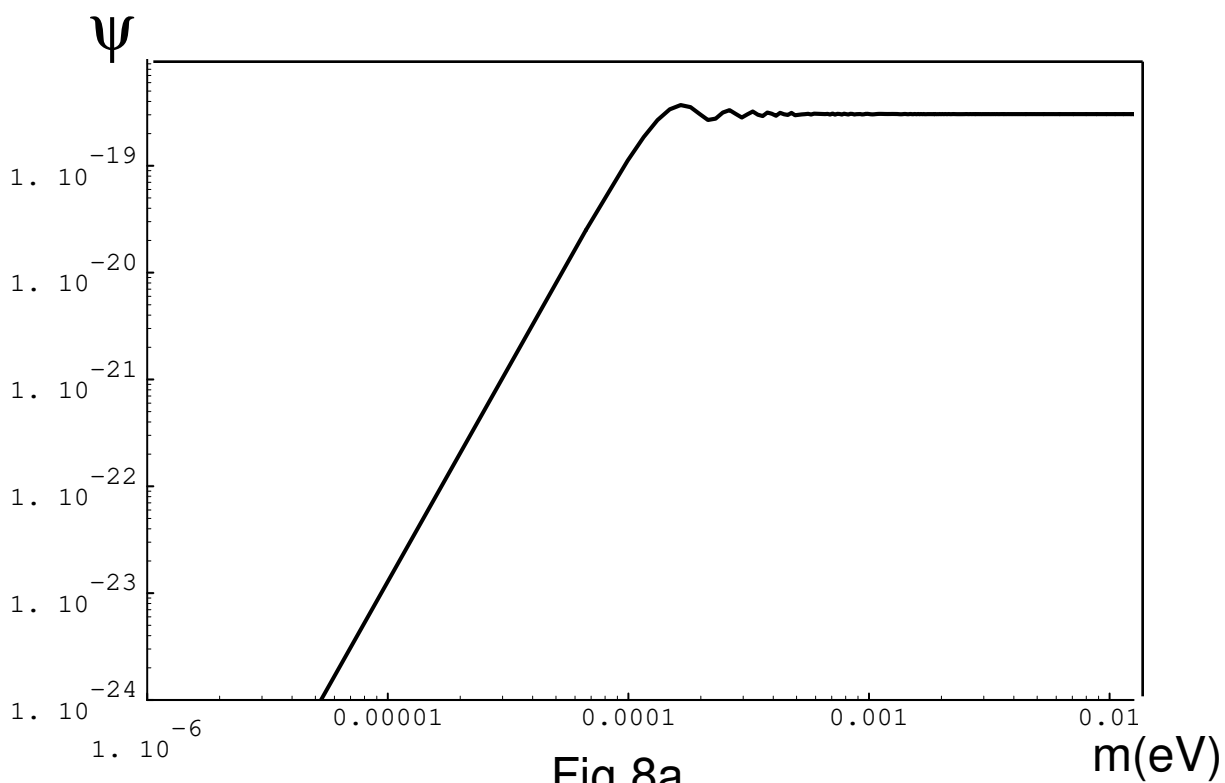


Fig.8a

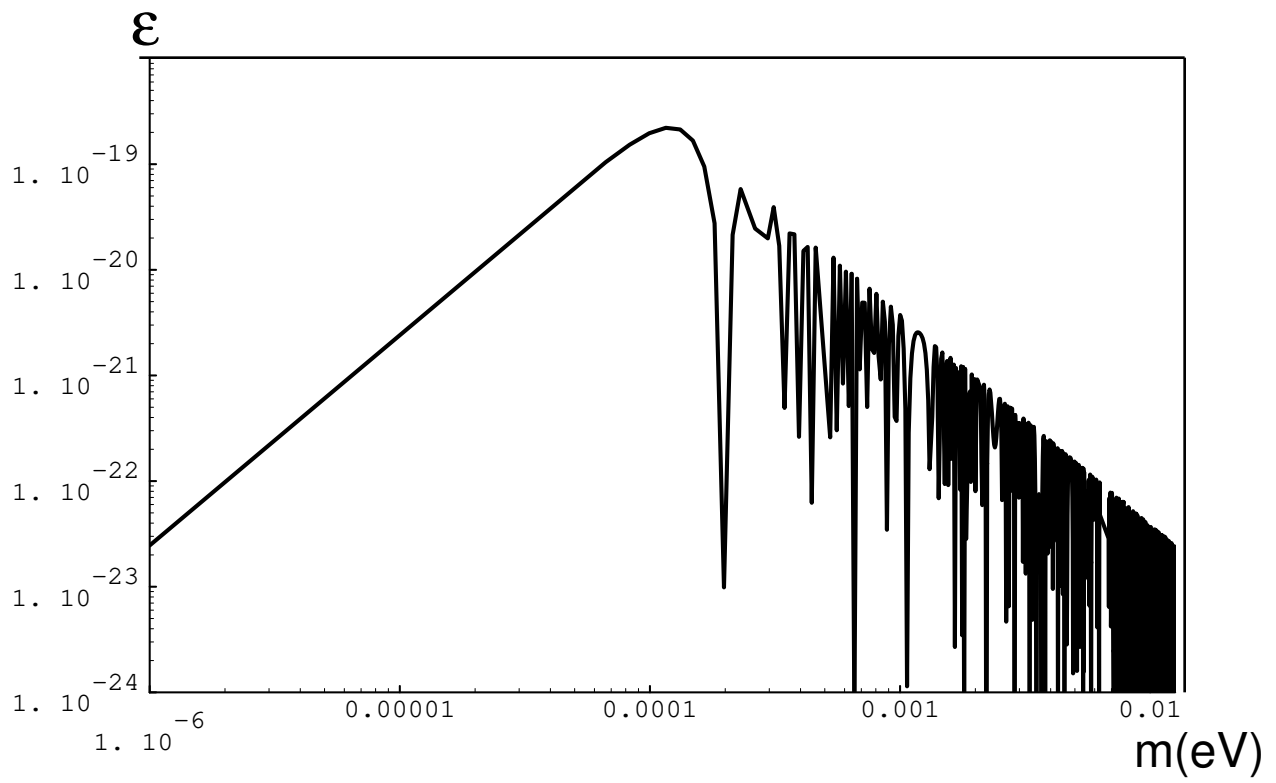


Fig.8b

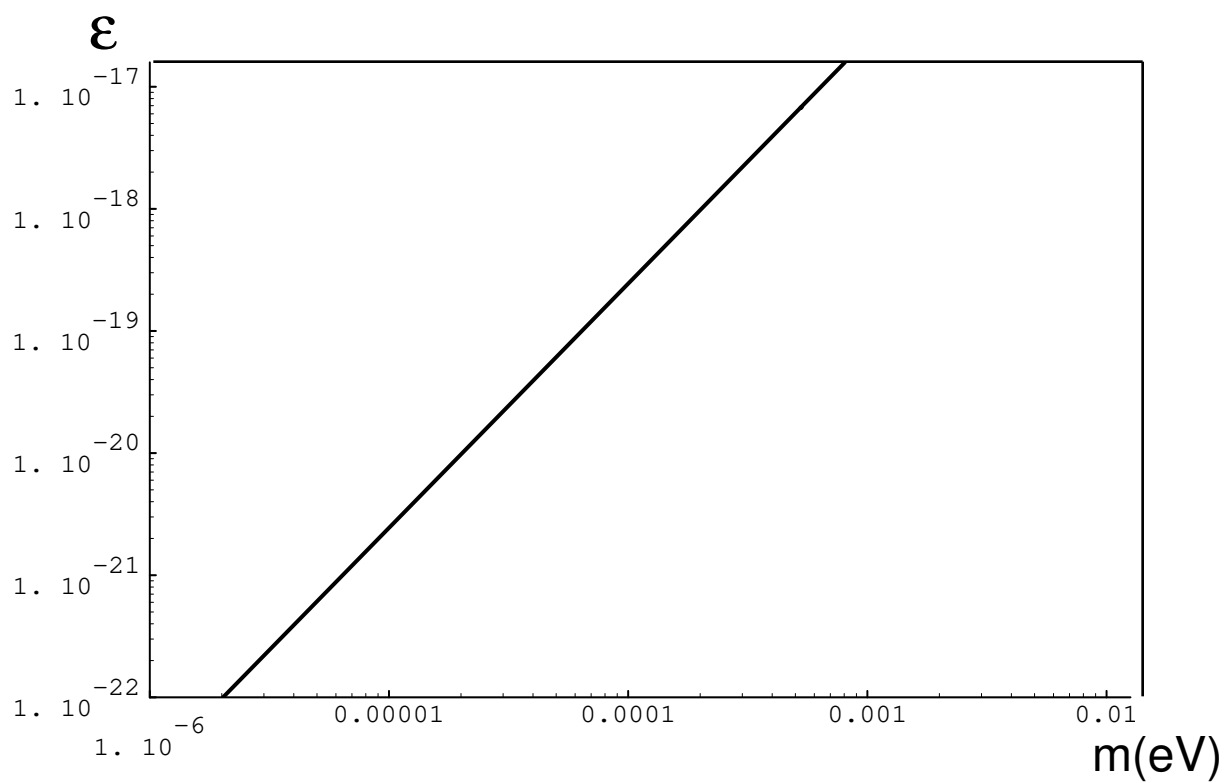


Fig.8c

This figure "fig1-8.png" is available in "png" format from:

<http://arxiv.org/ps/hep-ph/9409251v1>

This figure "fig1-9.png" is available in "png" format from:

<http://arxiv.org/ps/hep-ph/9409251v1>

This figure "fig1-10.png" is available in "png" format from:

<http://arxiv.org/ps/hep-ph/9409251v1>

This figure "fig1-11.png" is available in "png" format from:

<http://arxiv.org/ps/hep-ph/9409251v1>

This figure "fig1-12.png" is available in "png" format from:

<http://arxiv.org/ps/hep-ph/9409251v1>

This figure "fig1-13.png" is available in "png" format from:

<http://arxiv.org/ps/hep-ph/9409251v1>